Rapid *ESKAPE* Pathogens Detection Method using Tapered Dielectrophoresis Electrodes *via* Crossover Frequency Analysis

(Kaedah Pengesanan Pantas Patogen *ESKAPE* menggunakan Elektrod Dielektroforesis Tirus melalui Analisis Frekuensi Pindah Silang)

MUHAMMAD KHAIRULANWAR ABDUL RAHIM*, NUR MAS AYU JAMALUDIN, JACINTA SANTHANAM, AZRUL AZLAN HAMZAH & MUHAMAD RAMDZAN BUYONG

ABSTRACT

This paper introduces the versatile of an electrokinetic technique by using the non-uniform electric field for dielectrophoresis (DEP) application. This technique is defined as electromicrofluidics. The potential application for portable and real time detection method of Enterococcus faecium (EF), Staphylococcus aureus (SA), Klebsiella pneumoniae (KP), Acinetobacter baumannii (AB), Pseudomonas aeruginosa (PA) *and* Enterobacter aerogenes (EA), *which are the* (ESKAPE) *bacteria. The MATLAB analytical modelling was used in simulating the polarisation factor and velocities of bacteria based on Clausius-Mossotti factor (CMF). The validation of CMF simulation through the DEP experimental can be quantified based on the response of alternating current (AC) voltage applied using 6 voltage peak to peak (V_{p-p}) to their input frequencies from 100 to 15000 kHz. The droplet method was deployed to place properly 0.2 μL of sample onto DEP microelectrode. The velocities and crossover frequency (f_{xo}) ranges of bacteria were determined through bacteria trajectory in specific time interval monitored by microscope attached with eyepiece camera. The applied range of input frequencies from 100 to 15000 kHz at 6 (V_{p-p}) for each bacteria were successfully identified the unique ranges of frequencies response for detection application. The advantages of this works are selective with rapid capability for multidrug resistant (MDR) bacteria detection application.*

Keywords: Crossover frequency (f_{xo}); dielectrophoresis; ESKAPE bacteria

ABSTRAK

Makalah ini memperkenalkan satu teknik elektrokinetik yang menggunakan medan elektrik secara tidak seragam iaitu dielektroforesis (DEP). Teknik ini ditakrifkan sebagai elektromikrofluidik. Berpotensi bagi aplikasi secara mudah alih dan pada masa nyata untuk pengesanan Enterococcus faecium (EF), Staphylococcus aureus (SA), Klebsiella pneumoniae (KP), Acinetobacter baumannii (AB), Pseudomonas aeruginosa (PA) *dan* Enterobacter aerogenes (EA) *yang merupakan bakteria* (ESKAPE) *Pemodelan analitik MATLAB digunakan dalam mensimulasi faktor polarisasi dan halaju bakteria berdasarkan faktor Clasius-Mossotti (CMF). Pengesahan simulasi CMF melalui uji kaji DEP dapat dihitung berdasarkan tindak balas voltan arus ulang alik (AC) yang menggunakan 6 volt puncak ke puncak (V_{p-p}) terhadap frekuensi inputnya dari 100 sehingga 15000 kHz. Kaedah titisan digunakan untuk menempatkan 0.2 μL sampel ke atas permukaan mikroelektrod DEP dengan tepat. Julat halaju dan frekuensi pindah silang (f_{xo}) bakteria ditentukan melalui lintasan bakteria dalam selang waktu tertentu yang dipantau oleh mikroskop yang diintegrasikan bersama kamera. Julat frekuensi input yang dikenakan terhadap* ESKAPE *bakteria dari 100 hingga 15000 kHz pada 6 (V_{p-p}) untuk setiap bakteria berjaya dikenal pasti julat frekuensi pindah silang uniknya sebagai pengesanan. Hasil analisis, kelebihan penyelidikan ini adalah kebolehan secara selektif dengan kemampuan pantas untuk aplikasi pengesanan bakteria yang rentan kepada antibiotik (MDR),* ESKAPE *Ini membolehkan aplikasi pengesan bakteria ini dilakukan secara tepat dengan menggunakan teknik yang mudah pada masa hadapan.*

Kata kunci: Dielektroforesis; ESKAPE bakteria; frekuensi pindah silang (f_{xo})

INTRODUCTION

Over 40 years ago, dielectrophoresis (DEP) technology related to electrokinetic mechanism were explored. Recently, enhancement with integrated microelectrofluidic applications was established. The DEP microelectrofluidic solution is used for the detection, separation, and isolation of biology particles (Buyong et al. 2019; Yunus et al. 2019), bacteria (Rahim et al. 2018), red blood cells (RBC) (Abd Samad et al. 2019; Yunus et al. 2018), and

cancer cells (Jamaludin et al. 2018). Advantages, it is a contactless, simple, free contamination and clean method that uses non-uniform electric field expose to sample without additional of labelling material (Buyong et al. 2019; Cha et al. 2019; D'Amico et al. 2017; Kikkeri et al. 2018; Mohammad et al. 2017; Sadeghian et al. 2017; Shirmohammadli & Manavizadeh 2018; Siebman 2018).

This study was focused on DEP mechanism implementation for bacteria detection of the *Enterococcus faecium* (*EF*), *Staphylococcus aureus* (*SA*), *Klebsiella pneumonia* (*KP*), *Acinetobacter baumannii* (*AB*), *Pseudomonas aeruginosa* (*PA*) and *Enterobacter aerogenes* (*EA*). These bacteria are commonly associated to multidrug resistance (MDR) species (Brooks et al. 2018; González-Bello 2017; Karlowsky et al. 2017; Phoon et al. 2018; Rani et al. 2017; Santajit & Indrawattama 2016). The *ESKAPE* bacteria are divide into two groups; gram-positive and gram-negative. The gram-positive group includes *EF* and *SA* species. The *EF* species have round shape in pairs or chain arrangement. The SA species also have a round shape, but with grape-like cluster arrangement. The gram-negative group includes *KP*, *AB*, *PA* and *EA*. The *KP* is encapsulated and rod in shape. Meanwhile, *AB* has a rod shape and sometimes round when entering growing stages. The *PA* is rod in shape. Whereas the *EA* is gram-negative, rod in shape, and sometimes encapsulated.

Various methods have been developed by scientists for detecting bacteria produced by bacteria especially anti-resistance multidrug bacteria like *ESKAPE*. Additionally, there are several methods to rapidly detect *ESKAPE* bacteria. The current method for detecting *ESKAPE* bacteria is time consuming and complex (Santajit & Indrawattama

2016). The latest *ESKAPE* detection methods include mass spectrometric analysis (Leung et al. 2017), nitroreductase-triggered fluorescence turn-on probe (NTR) (Xu et al. 2017), T2 bacteria magnetic resonance assay (De Angelis et al. 2018) and isothermal DNA-based assays in a portable degas-actuated microfluidic diagnostic assay platform (Renner et al. 2017). All detection techniques require various steps prior to testing the samples. The Leung et al. (2017) method used the mass spectrometric analysis requires added chemical named ammonium-isobutyrate to isolate *ESKAPE* bacteria from pure culture or biological specimen to their whole cell lipids. This chemical is important in identifying the unique 'signature ions' of each *ESKAPE* species from their lipid cells by mass spectrometer. Xu et al. (2017) used the NTR technique which also requires additional chemical known as astris buffer solution at pH 7.4, containing 500 mM NADH for identifying all *ESKAPE* species with fluorescence analysis (FL analysis). Similar to these, Renner et al. (2017) technique also uses FL analysis, but the difference is that the method uses embedded electronics device with electronics circuit, battery, LEDs, and microfluidic channel. Different LEDs produce different intensity of fluorescence effect. This Renner et al. (2017) technique also uses FL intensity to identify *ESKAPE* bacteria, but it requires a reagent as additional chemical, which is magnesium acetate (MgOAc), during the sample loading step. De Angelis et al. (2018) technique is slightly different than the other methods discussed since it uses magnetic field to identify *ESKAPE* bacteria, but needs additional materials like superparamagnetic particles through the binding of attached species-specific probes.
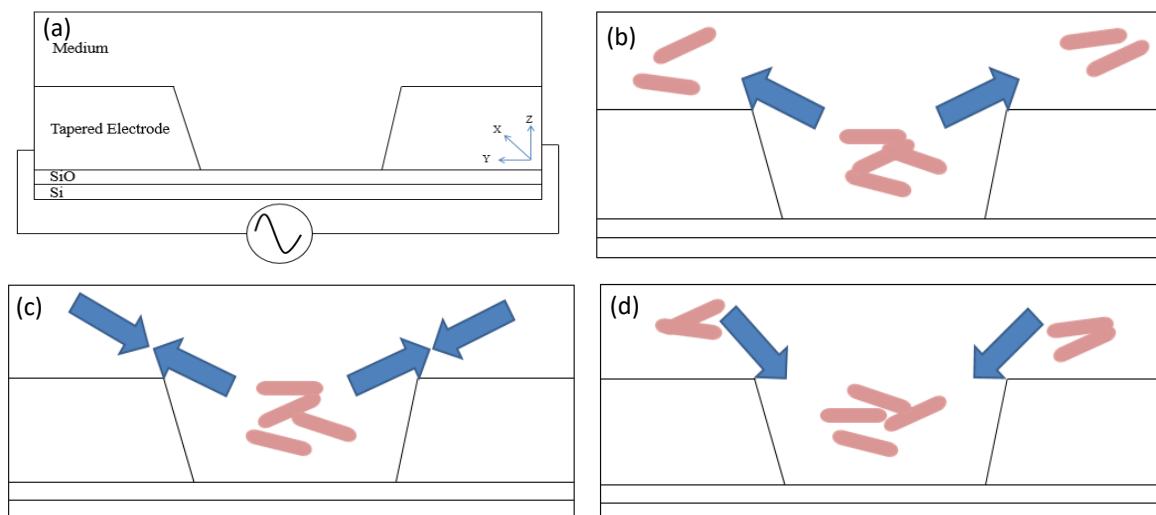

FIGURE 1. a) Schematic of DEP microelectrode configuration and blue arrows of lateral and vertical F_{DEP}, b) The *ESKAPE* bacteria, rod shaped is laterally attracted to top surface of DEP microelectrode when P_{DEP} frequency applied, c) No movement of *ESKAPE* bacteria when applying frequency P_{DEP} equivalent to N_{DEP} at f_{xo} value, and d) The *ESKAPE* bacteria is vertically repelled from the top surface of DEP microelectrode to center of channel when N_{DEP} frequency applied

The introduction of DEP technique is simple and clean method compared to other method. Not require any added chemical or materials, besides being a contactless method. Furthermore, it is able to give a rapid real time detection and easy to use. The novelty of the proposed technique is using tapered DEP microelectrode. Lateral and vertical DEP forces (F_{DEP}) were created by tapered DEP microelectrode, which made it easier to produce the isolation and selection of targeted *ESKAPE* bacteria. Thus, it is a potentially alternative solution for *ESKAPE* detection that is rapid and in real time. Figure 1 illustrates the schematic of DEP experimental and DEP responses positive DEP (P_{DEP}), negative DEP (N_{DEP}), and crossover frequency (f_{xo}).

DEP PRINCIPLE

There are several types of force manipulation and separation technique, but this paper related to DEP manipulation and separation technology for *ESKAPE* detection. Based on the literature review, the common types of force are electrics, magnetic, optical, and both electrics & magnetic as tabulated in Table 1. The electric force used in this study was DEP. The DEP is a type of electrokinetic technique that can conduct contactless manipulation and separation of particles using non-uniform electric field intensity (Pethig 2017). The magnetic resonance is a type of magnetic field manipulation. This method uses the superparamagnetic particles to bind with specific targeted bacteria in the presence of external magnetic field. The superparamagnetic particles act as bio tagging material to targeted bacteria, whereas the external magnetic field can create magnetic dipole moment when exposed to the superparamagnetic material and

targeted bacteria. Only the specific targeted bacteria can get through the separation channel containing seven channels with specific probes for each. These specific probes are useful for detecting and counting the number of bacteria isolated (De De Angelis et al. 2018). Another type of force is optical force. Generally, this technique uses different intensity of fluorescence with specific bio tagging material or some polymer chains to identify the targeted bacteria or bacteria. The rate of absorption and reflected fluorescence is detected by photodiode and measured to estimate the number of bacteria isolated (Renner et al. 2017; Xu et al. 2017). Lastly, the mass spectrometry invented by Leung et al. (2017) use a combination of the electric and magnetic forces. The *ESKAPE* sample in this technique was isolated from pure culture or biological specimen and whole cell lipids were extracted by hot ammonium isobutyrate. The lipid extracts were purified and analysed by MALDI-TOF-MS (mass spectrometry). A sample in liquid formed was ionised by bombarding it with electrons. The high energy of electron beam caused the *ESKAPE* bacteria solution with lipid polymerised molecules to break into charged fragments and charged non-fragments. The electric and magnetic field were subjected to these ions of *ESKAPE* bacteria solution, which were then separated according to their mass-to-ratio. The heavier ions were not or less deflected compared to the lighter ones. Electron multiplier acts as detector of charged ions. It can differentiate the different ions based on their mass. The results of function of the mass-to-charge ratio were obtained by the signal intensity of detected ions in which the characteristics of fragmentation pattern were known by correlating the masses of an entire molecule to the identified masses.

TABLE 1. Comparative analysis for difference type's force of manipulation technique

Type forces	Examples	Operation	References
Electrics	Dielectrophoresis	Dielectric polarity	(Pethig 2017)
Magnetics	Magnetic resonance	Intensity of magnetic field	(De Angelis et al. 2018)
Optical	Fluorescence analysis	Intensity of light	(Renner et al. 2017) (Xu et al. 2017)
Electrics and magnetics	Mass spectrometer	Mass of ions	(Leung et al. 2017)

This study emphasizes on finding f_{xo} from the basic formula of F_{DEP}. This enabled the differentiation and identification of the Clausius-Mossotti factor (CMF) for each *ESKAPE* species. The basic formula (1) of F_{DEP} can be written as:

$$F_{DEP} = 2\pi R^3 \varepsilon_m \varepsilon_0 \left(\frac{\varepsilon_p - \varepsilon_m}{\varepsilon_p + 2\varepsilon_m} \right) \nabla E^2 \qquad (1)$$

The R is particles radius, the polarisation factor or CMF is $(\frac{\varepsilon_p - \varepsilon_m}{\varepsilon_p + 2\varepsilon_m})$, ε_m is permittivity of medium, ε_p is permittivity of particles and the is the gradient of squared electric's field strength (Gascoyne et al. 2013; Honegger & Peyrade 2013; Pethig 2013). At the very low frequency of the current and voltage phasors are in phase (Pethig 2013). Thus, the conduction is dominance through the membrane. The conduction behaviour makes it easy for the medium to experience joule heating. Due to high conductivity, it can create bubbles in the medium. On the other hand, at very high frequency, the current phasor leads the voltage phasor by $\frac{\pi}{2}$ rad, making the permittivity parameter of cell more dominant compared to conductivity. High electrical charge stored in cell and medium can also cause the formation of bubbles (joule heating). At high frequency above than 100 kHz can reduce electrochemistry reaction (electrolysis) that caused the formation of bubbles (Adekanmbi & Srivastava 2019). Meanwhile, stated that at frequency range from 100 kHz to a few MHz, the electrothermal effect is raised due to increasing frequency range, which also causes joule heating (Du & Manoochehri 2008). This means that the input frequency above a few MHz can also cause the formation of bubbles. The CMF magnitude polarisation represents *ESKAPE* pathogen velocity. The transition CMF was from P_{DEP} to N_{DEP}, which was divided into two regions; positive region of P_{DEP} where particle is more polarised then medium and negative region (N_{DEP}) where particle is less polarised then medium. Meanwhile, at the f_{xo} point, the polarisation of P_{DEP} or N_{DEP} of particle was equal to polarisation of medium. The positive region, initially at low frequency, has high magnitude of P_{DEP}, represent that the velocity of *ESKAPE* pathogen was also

high. As the input frequency increases, the magnitudes of CMF decreased together with the velocity of *ESKAPE* pathogen. When it reached 0 magnitude of CMF, the P_{DEP} became equal to N_{DEP}, meaning that there was no movement of *ESKAPE* bacteria and velocity. The frequency increased after f_{xo} became 0 starting from the lowest magnitude of CMF until it reached the highest magnitude of CMF. It also increased the magnitude of the *ESKAPE* velocity for negative regions.

MATERIALS AND METHODS

FABRICATION PROCESS

The fabrication process technology of complementary metal-oxide-semiconductor (CMOS) is used in fabricated the Tapered Aluminium Microelectrode Arrays (TAMA) platform (Buyong et al. 2015). The plasma-enhanced chemical vapour deposition (PECVD) silicon oxide (SiO_2) is deposited about 1.15 μm as an insulator on top layer of silicon substrate. Then, the physical-vapour-deposition (PVD) technique is using to deposited about 60/30 nm of a thin adhesion layer of titanium/titanium nitrite (Ti/TiN). The PVD is using to deposited following the Ti/TiN deposition a layer of aluminium/silicon/copper Al/Si/Cu (98/1/1 wt. %) with thickness of 4.0 μm. To pattern the square array structure to the Al/Si/Cu layer, photolithography with resist thickness of 4.0 μm including UV cured for hardened photoresist process is performed. Lastly, by using inductive coupled plasma (ICP) etcher with advance plasma resist strip, Al/Si/Cu is being etched. The process flow of fabrication steps is presented in Figure 2(a) until 2(f).
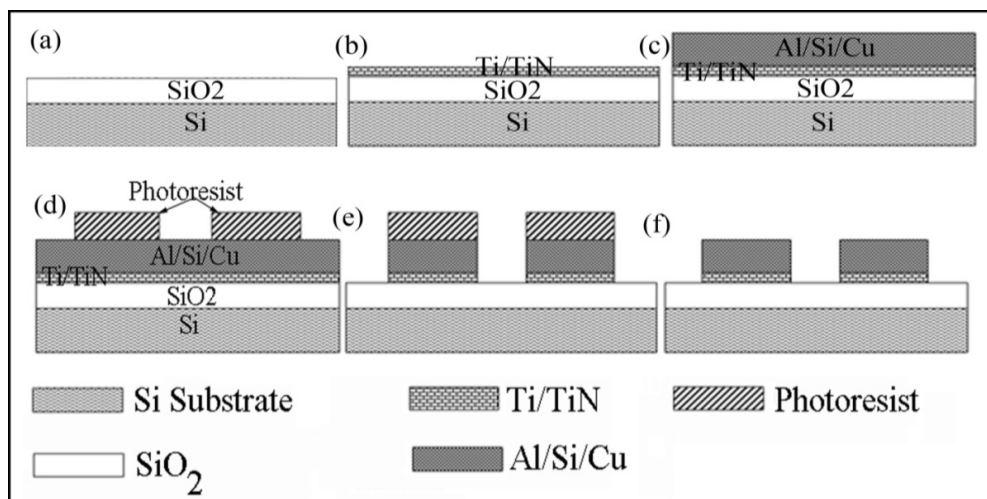

FIGURE 2. Schematic of process flow for TAMA fabrication (Buyong et al. 2019)

ESKAPE SAMPLES PREPARATION

The *ESKAPE* pathogens were obtained from the Novel Antibiotic Laboratory at the Faculty of Health Sciences, Universiti Kebangsaan Malaysia Kuala Lumpur (UKMKL) in formed culture petri dish. The first step of sample preparation is started by sterilising all equipment such as wire loop and agar petri dish that contain individual colonies of *ESKAPE* bacteria using the Bunsen burner. The wire loop was heated up until it looks like 'red flammable' and then, the temperature was reduced in a few seconds. After that, the white spot on the agar dish was scratched directly. The white spot was gently scratched only on the surface. The flame of Bunsen burner was retained open to ensure that the environment was still in a sterilised condition while making the bacteria suspension medium. Subsequent, the tiny dot of white spot was transferred from the agar incubated dish to the test tube containing 1 mL DI water. The DI water was stirred with wire loop inside the test tube until all tiny white spots on the wire loop were completely dissolved. The DI water with low permittivity of 78 F m^{-1} and conductivity of 0.0002 S m^{-1} was used for medium bacteria suspension preparation to reduce the joule heating effect. The wire loop was then removed and the cap of the test tube was immediately closed. The test tube was gently shaken to ensure that the bacteria suspension was completely dissolved.

ANALYTICAL MODELLING

The analytical modelling of polarisation factors is using Maxwell–Wagner effect for CMF analysis. The analytical modelling from complex number for extraction unique identifications of *ESKAPE* was done using MATLAB software. The analytical modelling of *ESKAPE* was derived from dielectric properties of *ESKAPE* and medium permittivity and conductivity values. The dielectric properties of permittivity and conductivity values are defined using the f_{xo} for all *ESKAPE* species.

DEP EXPERIMENTAL WORK

Based on the DEP experimental work, the physiological state of *ESKAPE* bacteria can be translated into dielectric properties to determine the F_{DEP}, P_{DEP} or N_{DEP} responses and the f_{xo}. Therefore, the analytical modelling CMF was validated by experimental DEP using tapered DEP microelectrode, TAMA to observe the actual of *ESKAPE* bacteria by observing P_{DEP}, N_{DEP}, and f_{xo} responses. Determination of range f_{xo} based on equation (1) use for *ESKAPE* bacteria detection, where the f_{xo} is related to F_{DEP} of P_{DEP} is equal to N_{DEP}. Once input frequency applied are increased or decreased in non-uniform electric field distribution, F_{DEP} responses will expose to *ESKAPE* bacteria cause the movement at different velocity. At certain frequency range, if there is no *ESKAPE* bacteria movement then it is defined as f_{xo}.

The experimental setup consisted of microscope (STM-6 Olympus Japan), eyepiece camera (AM7025X Dino-Eye Edge), function generator (IWATSU SG-4105), micro glass covers with dimension of 20 × 20 mm, prober, and tapered DEP microelectrode. The micropipette was used to drop 0.2 μL of *ESKAPE* bacteria suspension on tapered DEP microelectrode with polymide well having 2080 × 2080 μm of dimension. Micro cover glass was put on top of the DEP microelectrode to ensure that the *ESKAPE* bacteria droplets were properly confined. The DEP experimental setup for *ESKAPE* bacteria detection is illustrated in Figure 3.
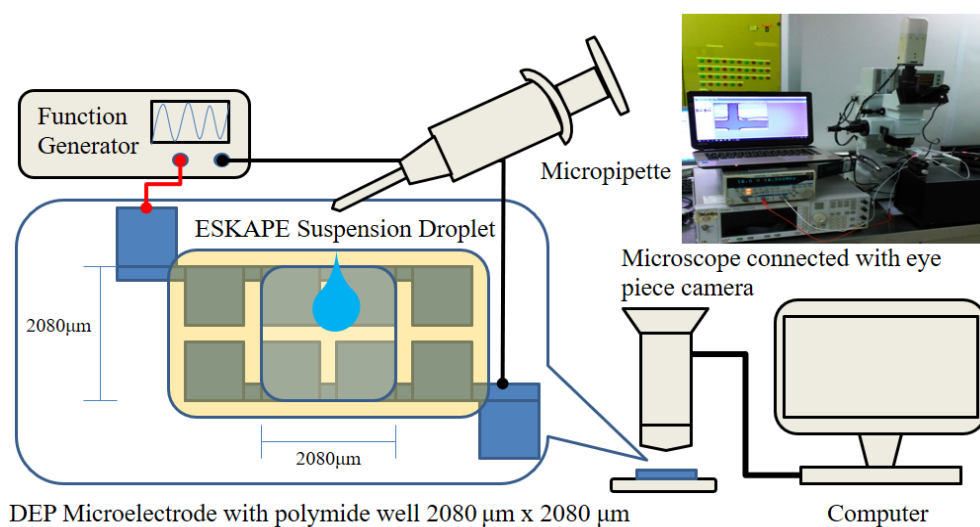

FIGURE 3. The illustration of DEP experimental setup for *ESKAPE* detection

MEASUREMENT OF *ESKAPE* VELOCITY

The measurement of *ESKAPE* velocity was based on video recording captured by eye-piece camera. From the video frame, the displacement of *ESKAPE* pathogen was identified with recorded time for velocity measurement analysis. The displacement between two points was done under condition P_{DEP} and N_{DEP}. In detail, for the case of P_{DEP}, the displacement range was 5 μm between of two microelectrode edges, which was to the top surface microelectrode. In contrast, N_{DEP} was from top surface of microelectrode to edges in between microelectrode with the similar displacement of 5 μm.

RESULTS AND DISCUSSION

ANALYTICAL CMF MODELLING

Based on the analytical modelling of CMF simulation, the detection frequency range was used from 100 until 15000 kHz, showed in Figure 4. The physical differences *ESKAPE* bacteria produced different frequency response. This is proven by referring f_{xo} differences for each *ESKAPE* bacterium. Equation (1) was use to identify values of each *ESKAPE* CMF . The CMF calculations are based on the parameter of shape and ranges size as tabled in Table 2. The unit of round-shaped bacteria was measured in μm as diameter meanwhile for rod-shaped bacteria were measured as a dimension of length by width, also the unit in μm.

TABLE 2. The ranges size/ dimension of *ESKAPE* pathogens

Pathogens species	Shape	Size/Dimension in μm	References
EF	Round	~ 0.75 - 0.76	(Lalam et al. 2015)
SA	Round	~ 0.50 - 1.00	(Gnanamani et al. 2017)
KP	Rod	~ 1.29 × 0.58	(Rajeshwari et al. 2009)
AB	Rod	~1.50-2.50 ×~1.00-1.50	(Almasaudi 2018)
PA	Rod	~ 2.0 × 0.50	(Vater et al. 2014)
EA	Rod	~ 1.45 × 0.70	(Diene et al. 2013)
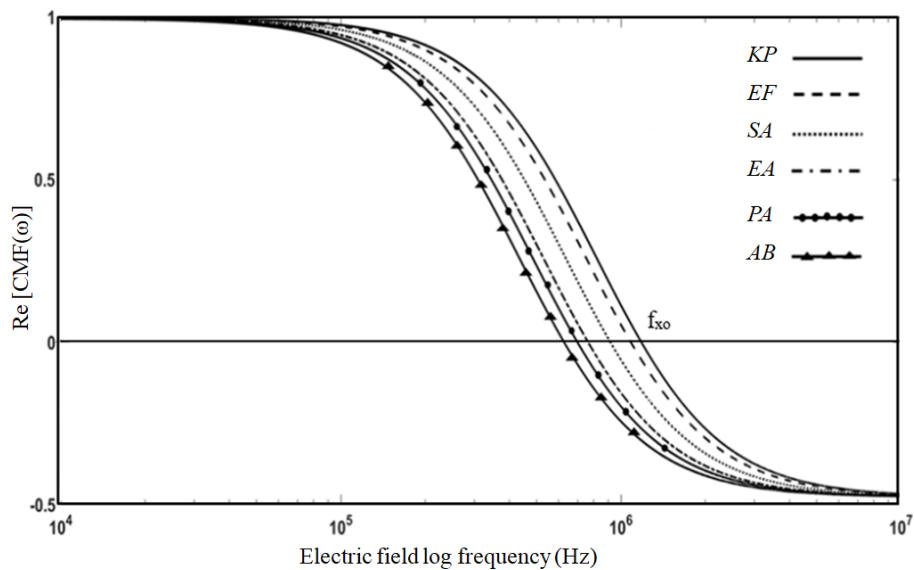
FIGURE 4. MATLAB simulation of CMF for *ESKAPE* bacteria

EXPERIMENTAL RESULT

This study has successfully conducted the DEP experiment for all six species of the *ESKAPE* bacteria. The f_{xo} ranges of *EF, SA, KP, AB, PA,* and *EA* were 11000 to 11100 kHz, 6000 to 10000 kHz, 7100 kHz, 6100 to 7000 kHz, 10000 to 12000 kHz, and 1200 to 1300 kHz, respectively. Meanwhile, the P_{DEP} range responses for *EF, SA, KP, AB, PA,* and *EA* were at 900 to 10900 kHz, 100 to 5900 kHz, 100 to 7000 kHz, 100 to 6000 kHz, 100 to 9900 kHz, and 300 to 1100 kHz, respectively. For N_{DEP} responses of *EF, SA, KP, AB, PA,* and *EA*, their input frequencies were 11200 to 15000 kHz, 11000 to 14000 kHz, 7500 to 15000 kHz, 7500 to 10000 kHz, 13000 to 15000 kHz, and 1400 to 15000 kHz, respectively. It is proven that the tapered DEP microelectrode has the ability for detection of the *ESKAPE* bacteria. Based on their different sizes and shapes that formulated into f_{xo} of CMF consisted permittivity and conductivity then represent as dielectric properties. Figure 5 shows example of *EA* species, 5(a)–5(b) the P_{DEP} responses when applied 6 V_{p-p} at the 300 kHz frequency. P_{DEP} response occurred *EA* species were attracted to the top surface of tapered DEP microelectrode, due high intensity of electric field at the top surface of tapered DEP microelectrode compared to in between microelectrode. Since the *EA* species were more polarised then the medium at applied input frequency. Furthermore, Figure 5(c)-5(d) shows that 6 V_{p-p} at 5000 kHz was identified as N_{DEP} response. All *EA* species were repelled to the centre of the tapered DEP microelectrode. This region has the low intensity of electric field, resulted the *EA* species to accumulate in between the microelectrode. In this condition as applied input frequency *EA* species were less polarised then the medium. Figure 5(e)-5(f) shows that input applied of 6 V_{p-p} at 1200 kHz, no movement for all *EA* species because there was no difference in F_{DEP}. Which means that P_{DEP} was equal to N_{DEP}, defined as f_{xo} for *EA* species detection. The white arrows in Figure 5(a)-5(b) and Figure 5(c)-5(d) illustrate the movement of *EA* bacteria when electric field was applied at initial 0 s to final stage 10 s, respectively.
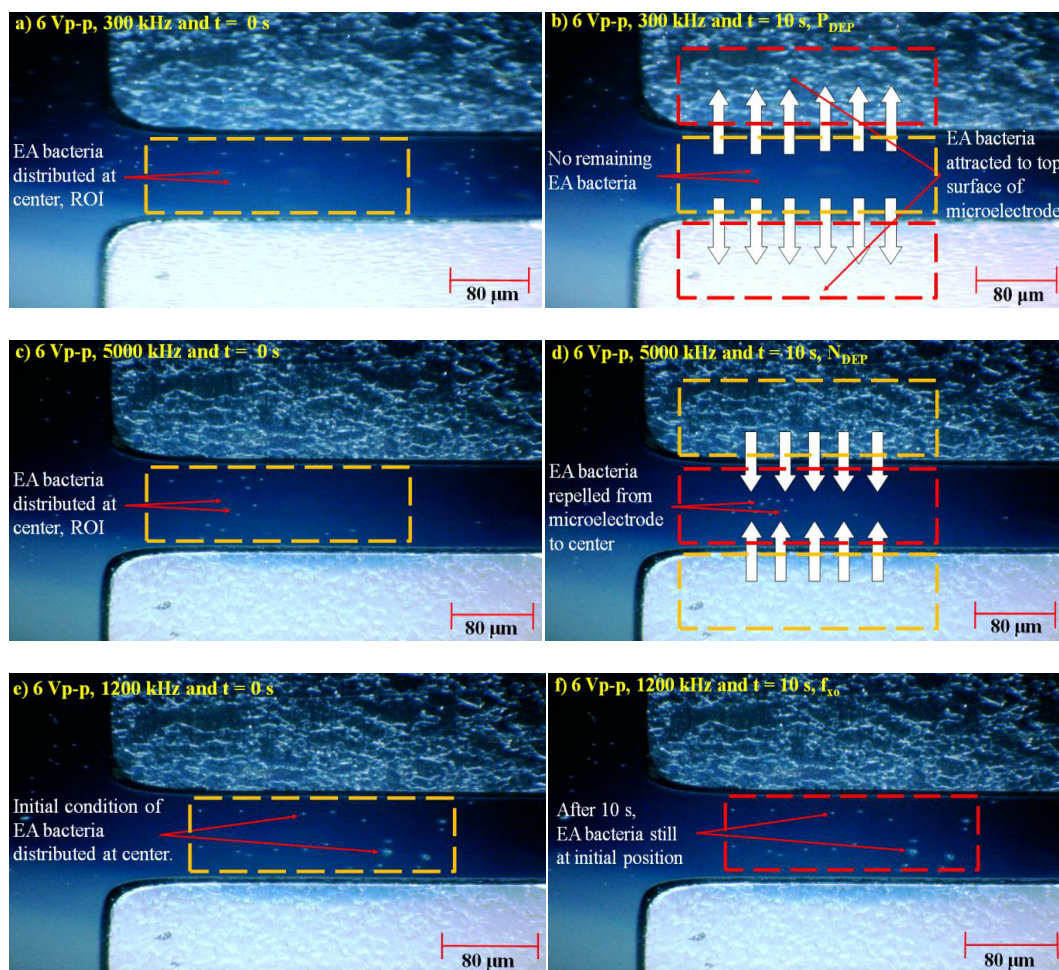

FIGURE 5. *EA* species (a) Initial condition at 6 V_{p-p} at 300 kHz, (b) P_{DEP} response after 10 s, (c) Initial condition at 6 V_{p-p} at 5000 kHz, (d) N_{DEP} response after 10 s, (e) Initial condition at 6 V_{p-p} at 1200 kHz, and (f) f_{xo} response, no movement after 10 s

ANALYSIS OF *ESKAPE* VELOCITY

Based on the DEP experimental, the velocity against input frequency curves for *ESKAPE* bacteria species were constructed as shown in Figure 6(a). The *EF* species showed five peaks for P_{DEP} and two peaks for N_{DEP}. The highest P_{DEP} velocity for *EF* was 3.81 μm s^{-1} at 200 kHz of input frequency, whereas the highest N_{DEP} velocity was 0.45 μm s^{-1} at 11800 kHz. The f_{xo} was determined when no movement of *EF* bacteria. The f_{xo} for *EF* was at the range of 11000 until 11800 kHz of input frequencies as shown in Figure 6(a). Subsequently, the *SA* species showed two peaks for P_{DEP} and one peak for N_{DEP}. The highest P_{DEP} velocity was 9.52 μm s^{-1} at 5000 kHz while the highest N_{DEP} velocity was 19.04 μm at 14000 kHz. The f_{xo} for *SA* species ranging from 6000 until 10000 kHz is as shown in Figure 6(a). The *KP* showed five peaks for P_{DEP} and two peaks for N_{DEP}. The highest P_{DEP} velocity was 4.39 μm s^{-1} at 2000 kHz while the highest N_{DEP} velocity was 0.24 μm s^{-1} at 7200 kHz. The f_{xo} was at 7100 kHz of input frequency as in Figure 6(a). The *AB* species showed five peaks for P_{DEP} and one peak for N_{DEP}. The highest P_{DEP} velocity was 5.85 μm s^{-1} at 3000 kHz while the highest N_{DEP} velocity was 0.40 μm s^{-1} at 7500 kHz. The f_{xo} of *AB* was ranged from 6100 until 7000 kHz. The *AB* curve is displayed in Figure 6(a). The *PA* species demonstrated four peaks for P_{DEP} and one peak for N_{DEP}. The highest P_{DEP} velocity was 12.4 μm s^{-1} at 3000 kHz and the highest N_{DEP} velocity was 0.28 μm s^{-1} at 13000 kHz. The f_{xo} for *PA* was ranged from 10000 until 12000 kHz as shown in Figure 6(a). Lastly, the *EA* species displayed one peak for P_{DEP} and one peak for N_{DEP}. The highest P_{DEP} velocity was 80 μm s^{-1} at 1100 kHz and the highest N_{DEP} velocity was 40 μm s^{-1} at range frequency of 8000 until 10000 kHz. Meanwhile, their f_{xo} frequency was ranged from 1200 until 1300 kHz. The *EA* velocity curve is as shown in Figure 6(a). From further analysis of velocity *ESKAPE* bacteria we can produce the secondary data and plotted the frequencies range for P_{DEP} and N_{DEP} in Figure 6(b). The P_{DEP} response for *EF* species is range in 100 until 11000 kHz and for N_{DEP} is range in 11800 until 15000 kHz. The *SA* species for P_{DEP} is range in 100 until 6000 kHz meanwhile for N_{DEP} is range in 10000 until 14000 kHz. The *KP* species for P_{DEP} is range in 100 until 7000 kHz but for N_{DEP} is range in 7200 until 15000 kHz. The *AB* species for P_{DEP} is range in 100 until 6100 kHz. Meanwhile, for N_{DEP} response is range in 7000 until 10000 kHz. The *PA* species for P_{DEP} is range in 100 until 10000 kHz and their N_{DEP} response is range in 12000 until 15000 kHz. Then, lastly the *EA* species for P_{DEP} is range in 100 until 1100 kHz. Meanwhile, for their N_{DEP} response is range in 1300 until 15000 kHz. Figure 6(b) is illustrated the working frequency range for P_{DEP} and N_{DEP} by left-right arrows. The coloured box was showed the f_{xo} ranges for each *ESKAPE* species. Based on the velocity curve in Figure 6(b), a step of determining a f_{xo} of two or more *ESKAPE* bacteria having over-lapping dielectrophoretic frequency responses, f_{xo} was defined. In the case of *SA*
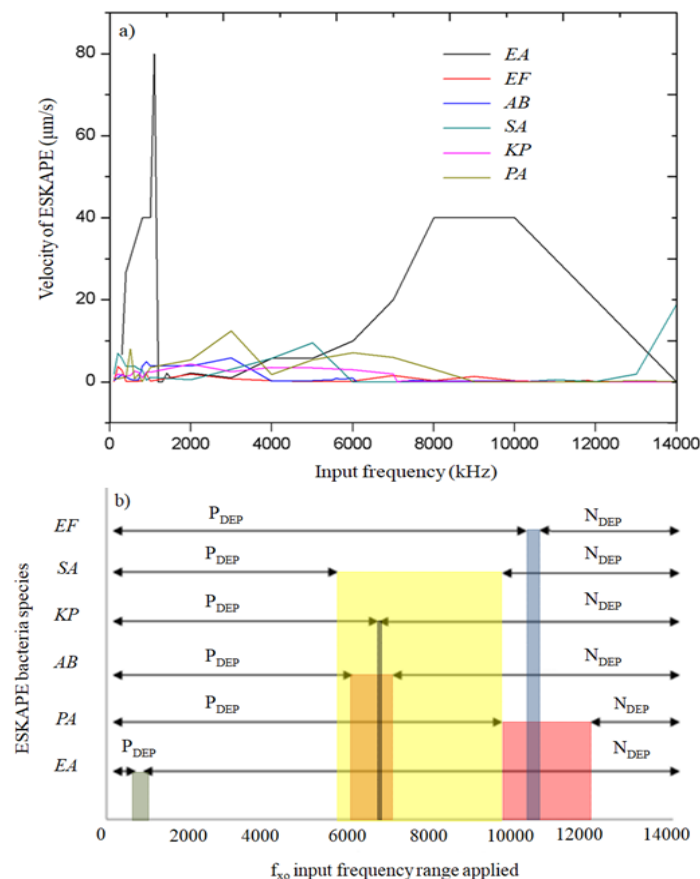

FIGURE 6. Experimental results for ESKAPE (a) Velocity of ESKAPE versus input frequency applied and (b) *ESKAPE* species versus f_{xo} detection of frequency range

and *KP*, the detection *KP* was easier because there was only one point of f_{xo}. However, for *SA* species there was a wide range of DEP crossover between 6000 and 10000 kHz. This is due to different physical size and shape of *SA* and *KP*, thus, different range of f_{xo} was produced. The *SA* species physically have round shape-grape arrangement (Gnanamani et al. 2017) and a wide frequency range as shown in this study. Based on the *SA* species bacteria cell arrangement, the total surface area was increased due to the grape-shaped arrangement. Thus, the equation of F_{DEP} proved that the dielectrics values were also increased. In contrast, the *KP* species have a rod shape but exist in individual arrangement (Rajeshwari et al. 2009). This has caused a low surface area compared to that of *SA* species. The dielectric values of *KP* were also decreased, which was proved by DEP experiment showing only one f_{xo} point at 7100 kHz. Furthermore, in this study three ESKAPE species namely *SA*, *KP,* and *AB* were overlapped at certain f_{xo} range points (7100 kHz and 6100 to 7000 kHz) as showed in Figure 6(b). The smallest range of the black box of *KP,* the medium of range of the brown box of *AB* were intercepted in bigger yellow box of *SA* due to bigger range of f_{xo}. Detection these three *ESKAPE* species using the lowest and highest ranges of f_{xo} were utilised by identified the uniqueness of their own different of dielectric properties for *ESKAPE* detection species. Similar method also is implemented to another three of *ESKAPE* species namely *PA* and *EF* were overlapped at certain f_{xo} also *EA* species.

DISCUSSION

The shape and size of each *ESKAPE* species was not identical. The average size of *ESKAPE* species was below 2 μm. In fact, range size of each *ESKAPE* species was between 1 and 2 μm. Therefore, based on the shape and size produced different dielectric values resulted unique f_{xo} for rapid *ESKAPE* bacteria detection method using tapered DEP microelectrodes via f_{xo} analysis. The results of maximum and average speed for each *ESKAPE* bacteria were listed in Table 3.

TABLE 3. Speed of movement and average speed of *ESKAPE* pathogens

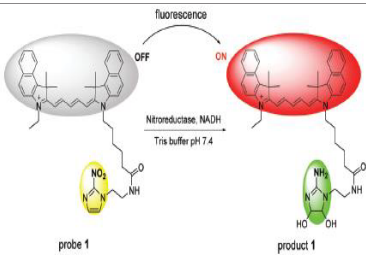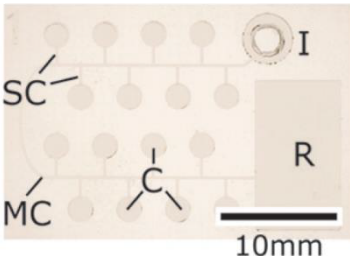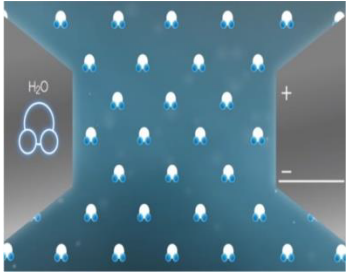| Species	Speed of movement (μm s^{-1})		Average of speed (μm s^{-1})
	P_{DEP} (max)	N_{DEP} (max)	
EF	3.81	0.45	2.13
SA	9.52	19.04	14.28
KP	4.39	0.24	2.31
AB	5.85	0.40	3.13
PA	12.4	0.28	6.34
EA	80	40	60

The higher speed movement of F_{DEP} response was *EA* species, 80 μm s^{-1} for P_{DEP}, and 40 μm s^{-1} for N_{DEP} with an average speed of 60 μm s^{-1}. Meanwhile, the lower speed movement is *EF* species with 3.81 μm s^{-1} for P_{DEP} and 0.45 μm s^{-1} for N_{DEP} with an average speed of 2.13 μm s^{-1}. The *EF* and *SA* bacteria have round-shaped and the smallest sizes compared to *KP*, *AB*, *PA*, and *EA* species. However, *EF* and *SA* velocities are lower because of the arrangement in colonies such as grape-like clusters and pair-chains. It makes heavier F_{DEP} for levitated these two species of bacteria *EF* and *SA*. The rest of the bacteria for four species *KP*, *AB*, *PA*, and *EA* are exited in individual orientation, not in colony form. In general, *KP*, *AB*, *PA*, and *EA* have rod-shaped with ranged dimensions were ~ 1.29 to 2.0 μm in length by ~ 0.50 to 1.50 μm in width. It was a larger range of sizes compared to *PA* and *SA* species. It also means that *KP*, *AB*, and *PA* have heavier F_{DEP} for levitate these kinds of bacteria. Special case for *EA*, there has the addition structure coved at the surface of the rod, it called pilus and flagella. It was like a hair structure, used for bacteria swimming and reproduction. The *EA* species existed in individual but the pilus and flagella make the bacteria attached to each other when the electric field applied in DEP experimental. Its surface area increases and make heavier. With the increasing value of frequencies, the effectiveness of F_{DEP} also increases then it can levitate the *EA* bacteria attached each with a larger surface area. Initially, it has low momentum due to low

frequencies range but after it achieved maximum F_{DEP} effectiveness at 1100 kHz of P_{DEP} and 8000 until 10000 kHz of N_{DEP}. Therefore, it generated the high momentum and then produced the maximum velocity of 80 $\mu m\ s^{-1}$ of P_{DEP} and 40 $\mu m\ s^{-1}$ of N_{DEP}, respectively. This proved each *ESKAPE* bacteria has a unique morphology that influenced their dielectric properties due to different shapes, sizes and arrangements. Meaning that when we are increasing or decreasing the input frequency value, this resulted in the differences of F_{DEP} responses based on each of *ESKAPE* dielectric properties. The experimental DEP result indicated that only *EA* species have the different f_{xo} range from 1200 until 1300 kHz compared to that of the other five species. This means that there was no intersection to other f_{xo} ranges of other five species *ESKAPE*. The *PA* species have f_{xo} range of 10000 to 12000 kHz, which intercepted f_{xo} *SA* and *EF* at 10000 kHz and 11000 to 11200 kHz, respectively. The *SA*, f_{xo} also intercepted *AB* at range of 6100 to 7000 kHz. The *SA* and *KP* were intercepted at 7100 kHz. Therefore, the species detection of mixtures for *EF* and *PA* species utilizes the maximum range of f_{xo} was used for *EF* followed by the minimum f_{xo} range for *PA*. Meanwhile for *SA* species detection, maximum f_{xo} was used. The *EA* species showed no intersection of f_{xo} to another five species of *ESKAPE*, suggesting that their f_{xo} range can be used directly as in Figure 6(b). The detecting *AB* and *KP* species was quiet challenging as their f_{xo} ranges overlapped to the huge *SA* f_{xo} range. Overall, DEP method is potentially and suitable for *ESKAPE* species detection method. However, further investigation on similar physical size and the f_{xo} need to be explore. Table 4 was listed and summarized all the *ESKAPE* species detection technique based on our discussions in the introduction section. The comparison DEP result was included the detection method, time constrain, and advantages and disadvantages.

TABLE 4. The comparison of current technologies used for *ESKAPE* bacteria detection with tapered DEP microelectrode technique

| Detection method	Time required	Advantages/ Disadvantages
Nuclear Imaging (Xu et al. 2017)	60 min	Advantages: i. Rapid detection Disadvantages: i. Required buffer solution ii. Complicated system
Optics imaging (Renner et al. 2017)	30 min	Advantages: ii. Rapid detection iii. Portable Disadvantages: i. Required solvent
Magnetic Resonance (De Angelis et al. 2018)	300min	Advantages: i. Automated Disadvantages: i. Marker tagging ii. Not portable iii. Expensive
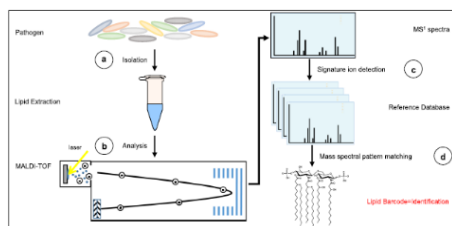
Electric and Magnetic (Leung et al. 2017)

Real time detection

Advantages:
  i.   Rapid detection

Disadvantage:
  i.   Required Solvent

  ii. Not portable
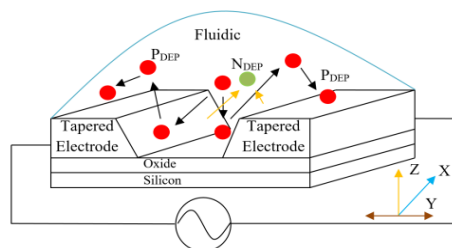
DEP (Buyong et al. 2019)

Real time detection

Advantages:
  i.   Rapid detection

  ii. No labelling

Disadvantages:
  i.   Required AC field

  ii. Joule Heating

  iii. Electrolysis

CONCLUSION

The DEP detection based on shape and size of *ESKAPE* bacteria were approximately average from 1 to 2 μm resulted in the f_{xo} overlap. Therefore, there was a wide frequency range observed due to different geometrical size and shapes of round and rod among the *ESKAPE* bacteria. The utilization of f_{xo} has overlapping differences, which have the potential to formulate the detection based on the lowest and highest ranges of f_{xo} for each *ESKAPE* bacteria. Thus, the f_{xo} were defined as potential solution for rapid *ESKAPE* bacteria detection method using tapered DEP microelectrodes via f_{xo} analysis.

ACKNOWLEDGEMENTS

REFERENCES

Abd Samad, M.I., Buyong, M.R., Kim, S.S. & Majlis, B.Y. 2019. Dielectrophoresis velocities response on tapered electrode profile: Simulation and experimental. *Microelectronics International* 36: 45-53.

Adekanmbi, E.O. & Srivastava, S.K. 2019. Applications of electrokinetics and dielectrophoresis on designing chip-based disease diagnostic platforms. *In Bio-Inspired Technology*. https://www.intechopen.com/books/bio-inspired-technology/applications-of-electrokinetics-and-dielectrophoresis-on-designing-chip-based-disease-diagnostic-pla. DOI: 10.5772/intechopen.82637.

Almasaudi, S.B. 2018. *Acinetobacter* spp. as nosocomial pathogens: Epidemiology and resistance features. *Saudi Journal of Biological Sciences* 25(3): 586-596.

Brooks, L.E., Ul-Hasan, S., Chan, B.K. & Sistrom, M.J. 2018. Quantifying the evolutionary conservation of genes encoding multidrug efflux pumps in the ESKAPE pathogens to identify antimicrobial drug targets. *Msystems* 3(3): 1-9.

Buyong, M.R., Kayani, A.A., Hamzah, A.A. & Majlis, B.Y. 2019. Dielectrophoresis manipulation: Versatile lateral and vertical mechanisms. *Biosensors* 9(30): 1-26.

Buyong, M.R., Larki, F., Faiz, M.S., Hamzah, A.A., Yunas, J. & Majlis, B.Y. 2015. Tapered aluminium microelectrode array for improvement of dielectrophoresis-based particle manipulation. *Sensors* 15(5): 10973-10990.

Cha, S.H., Kang, S.H., Lee, Y.J., Kim, J.H., Ahn, E.Y., Park, Y. & Cho, S. 2019. Fabrication of nanoribbons by dielectrophoresis assisted cold welding of gold nanoparticles on mica substrate. *Scientific Reports* 9(1): 1-12.

D'Amico, L., Ajami, N.J., Adachi, J.A., Gascoyne, P.R. & Petrosino, J.F. 2017. Isolation and concentration of bacteria from blood using microfluidic membraneless dialysis and dielectrophoresis. *Lab on a Chip* 17(7): 1340-1348.

De Angelis, G., Posteraro, B., De Carolis, E., Menchinelli, G., Franceschi, F., Tumbarello, M., De Pascale, G., Spanu, T. & Sanguinetti, M. 2018. T2 Bacteria magnetic resonance assay for the rapid detection of ESKAPEc pathogens directly in whole blood. *Journal of Antimicrobial Chemotherapy* 73(suppl_4): iv20-iv26.

Diene, S.M., Merhej, V., Henry, M., El Filali, A., Roux, V., Robert, C., Azza, S., Gavory, F., Barbe, V., La Scola, B. & Raoult, D. 2013. The rhizome of the multidrug-resistant Enterobacter aerogenes genome reveals how new 'killer bugs' are created because of a sympatric lifestyle. *Molecular Biology and Evolution* 30(2): 369-383.

Du, E. & Manoochehri, S. 2008. Electrohydrodynamic-mediated dielectrophoretic separation and transport based on asymmetric electrode pairs. *Electrophoresis* 29(24): 5017-5025.

Gascoyne, P.R., Shim, S., Noshari, J., Becker, F.F. & Stemke, H.K. 2013. Correlations between the dielectric properties and exterior morphology of cells revealed by dielectrophoretic field-flow fractionation. *Electrophoresis* 34(7): 1042-1050.

Gnanamani, A., Hariharan, P. & Paul-Satyaseela, M. 2017. *Staphylococcus aureus*: Overview of bacteriology, clinical diseases, epidemiology, antibiotic resistance and therapeutic approach. *Frontiers in Staphylococcus aureus* 2017: 4-28.

González-Bello. C. 2017. Antibiotic adjuvants - a strategy to unlock bacterial resistance to antibiotics. *Bioorganic & Medicinal Chemistry Letters* 27(18): 4221-4228.

Honegger, T. & Peyrade, D. 2013. Comprehensive analysis of alternating current electrokinetics induced motion of colloidal particles in a three-dimensional microfluidic chip. *Journal of Applied Physics* 113(19): 194702.

Jamaludin, N.M.A., Buyong, M.R., Rahim, M.K., Hamzah, A.A., Mailis, B.Y. & Bais, B. 2018. Dielectrophoresis: Characterization of triple-negative breast cancer using Clausius-Mossotti factor. In *2018 IEEE International Conference on Semiconductor Electronics (ICSE)* IEEE. pp. 85-88.

Karlowsky, J.A., Hoban, D.J., Hackel, M.A., Lob, S.H. & Sahm, D.F. 2017. Antimicrobial susceptibility of gram-negative ESKAPE pathogens isolated from hospitalized patients with intra-abdominal and urinary tract infections in Asia-Pacific countries: SMART 2013-2015. *Journal of Medical Microbiology* 66(1): 61-69.

Kikkeri, K., Breazeal, M.V.R., Ren, X., Pruden, A. & Agah, M. 2018. A monolithic dielectrophoresis chip with impedimetric sensing for assessment of pathogen viability. *Journal of Microelectromechanical Systems* 27(5): 810-817.

Lalam, C., Tantravahi, S. & Petla, N. 2015. Identification and characterization of *Enterococcus feacium* (MCC-2729) with antimicrobial and abiotic stress tolerance properties. *International Journal of Current Microbiology and Applied Science* 4(8): 309-322.

Leung, L.M., Fondrie, W.E., Doi, Y., Johnson, J.K., Strickland, D.K., Ernst, R.K. & Goodlett, D.R. 2017. Identification of the ESKAPE pathogens by mass spectrometric analysis of microbial membrane glycolipids. *Scientific Reports* 7(1): 1-10.

Mohammad, K., Buchanan, D.A., Braasch, K., Butler, M. & Thomson, D.J. 2017. CMOS single cell dielectrophoresis cytometer. *Sensors and Actuators B: Chemical* 249(2012): 246-255.

Pethig, R.R. 2017. *Dielectrophoresis: Theory, Methodology and Biological Applications*. 1st ed. London, Ontario: John Wiley & Sons. Inc. pp. 253-254.

Pethig, R. 2013. Dielectrophoresis: An assessment of its potential to aid the research and practice of drug discovery and delivery. *Advanced Drug Delivery Reviews* 65(11-12): 1589-1599.

Phoon, H.Y., Hussin, H., Hussain, B.M., Lim, S.Y., Woon, J.J., Er, Y.X. & Thong, K.L. 2018. Distribution, genetic diversity and antimicrobial resistance of clinically important bacteria from the environment of a tertiary hospital in Malaysia. *Journal of Global Antimicrobial Resistance* 14(2018): 132-140.

Rani, F.M., Rahman, N.I.A., Ismail, S., Alattraqchi, A.G., Cleary, D.W., Clarke, S.C. & Yeo, C.C. 2017. *Acinobacter* spp. infections in Malaysia: A review of antimicrobial resistance trends, mechanisms and epidemiology. *Frontiers in Microbiology* 8(2017): 1-13.

Rahim, M.K.A., Buyong, M.R., Jamaludin, N.M.A., Hamzah, A.A., Siow, K.S. & Majlis, B.Y. 2018. Characterization of permittivity and conductivity for ESKAPE pathogens detection. *IEEE International Conference on Semiconductor Electronics (ICSE)*. pp. 132-135.

Rajeshwari, H., Nagveni, S., Oli, A., Parashar, D. & Chandrakanth, K.R. 2009. Morphological changes of *Klebsiellapneumoniae* in response to cefotaxime: A scanning electron microscope study. *World Journal of Microbiology and Biotechnology* 25(2009): 2263-2266.

Renner, L.D., Zan, J., Hu, L.I., Martinez, M., Resto, P.J., Siegel, A.C., Torres, C., Hall, S.B., Slezak, T.R., Nguyen, T.H. & Weibel, D.B. 2017. Detection of ESKAPE bacterial pathogens at the point of care using isothermal DNA-based assays in a portable degas-actuated microfluidic diagnostic assay platform. *Applied and Environmental Microbiology* 83(4): e02449.

Sadeghian, H., Hojjat, Y. & Soleimani, M. 2017. Interdigitated electrode design and optimization for dielectrophoresis cell separation actuators. *Journal of Electrostatics* 86: 41-49.

Santajit, S. & Indrawattana, N. 2016. Mechanisms of antimicrobial resistance in ESKAPE pathogens. *BioMed Research International* 2016: 2475067.

Shirmohammadli, V. & Manavizadeh, N. 2018. Numerical modeling of cell trajectory inside a dielectrophoresis microdevice designed for breast cancer cell screening. *IEEE Sensors Journal* 18(20): 8215-8222.

Siebman, C., Velev, O. & Slaveykova, V. 2018. Probing contaminant-induced alterations in chlorophyll fluorescence by AC-dielectrophoresis-based 2D-algal array. *Biosensors* 8(1): 2-8.

Vater, S.M., Weiße, S., Maleschlijski, S., Lotz, C., Koschitzki, F., Schwartz, T., Obst, U. & Rosenhahn, A. 2014. Swimming behavior of *Pseudomonas aeruginosa* studied by holographic 3D tracking. *PloS ONE* 9(1): e87765.

Xu, S., Wang, Q., Zhang, Q., Zhang, L., Zuo, L., Jiang, J.D. & Hu, H.Y. 2017. Real time detection of ESKAPE pathogens by a nitroreductase-triggered fluorescence turn-on probe. *Chemical Communications* 53(81): 11177-11180.

Yunus, F.W., Buyong, M.R., Yunas, J., Majlis, B.Y. & Hamzah, A.A. 2019. 3-dimensional electric field distributions of castellated and straight dielectrophoresis electrodes for cell separation. *Sains Malaysiana* 48(6): 1239-1249.

Yunus, F.W., Hamzah, A.A., Norzin, M.S., Buyong, M.R., Yunas, J. & Majlis, B.Y. 2018. Dielectrophoresis: Iron deficient

anemic red blood cells for artificial kidney purposes. *IEEE International Conference on Semiconductor Electronics (ICSE)*. pp. 5-8.

Muhammad Khairulanwar Abdul Rahim*, Nur Mas Ayu Jamaludin, Azrul Azlan Hamzah & Muhamad Ramdzan Buyong
Institute of Microengineering and Nanoelectronics (IMEN)
Universiti Kebangsaan Malaysia
43600 UKM Bangi, Selangor Darul Ehsan
Malaysia

Jacinta Santhanam
Faculty of Health Sciences
Universiti Kebangsaan Malaysia
50300 Kuala Lumpur, Federal Territory
Malaysia

*Corresponding author; email: muhdramdzan@ukm.edu.my